

# Effect of planar anisotropy in vortex configuration of micro-scale disks

S. O. Parreiras<sup>1,2\*</sup> and M. D. Martins<sup>1†</sup>

<sup>1</sup>*LabNano, CDTN/CNEN, Belo Horizonte, Brazil*

<sup>2</sup>*UFMG, Belo Horizonte, Brazil*

*sofiaparreiras@gmail.com, mdm@cdtn.br*

## Abstract

The magnetic configuration of micron-sized  $\text{Co}_{60}\text{Fe}_{40}$  and Permalloy disks was investigated using micromagnetic simulations and magnetic force microscopy (MFM) measurements. By comparing both materials, it is possible to elucidate the effect of the planar magnetocrystalline anisotropy in the stability of the magnetic vortex configuration. The results for disks with diameters between 0.5 and 8  $\mu\text{m}$  showed that the magnetic anisotropy favors spins alignment and domains division, reducing vortex stability. Different magnetic configurations was observed for each disk diameter. Additionally, a statistical analysis of the magnetic configuration distribution experimentally observed by MFM was performed and compared with the simulation results.

*Keywords:* Magnetic vortex, planar anisotropy, micromagnetic simulations, magnetic force microscopy, statistical analysis

## 1 Introduction

A magnetic vortex has been observed as the ground state in many soft ferromagnetic materials in micro and submicron scales <sup>(1), (2)</sup>. For these materials, small changes in shape, size and anisotropy can modify the energy equilibrium that defines the stable spin structure <sup>(3)</sup>. Many technological applications have been proposed based on magnetic vortices, among these, the most promising applications involve the dynamic behavior of the vortex due to an external excitation. The vortex dynamic properties possibility its application ranging from spintronic devices, as spin-torque nano-oscillators (STNOs) <sup>(4), (5)</sup> and vortex random access memory (VRAM) <sup>(6), (7), (8)</sup> to biofunctionalized microdisks to destroy cancer cells <sup>(9), (10), (11)</sup>.

The vortex configuration in magnetic disks is characterized by a closed circuit of spins in the plane of the disk with a region near the center (the vortex core), where the spins are aligned perpendicularly to the plane. The direction of the core spins (up or down) determines the core polarity. When a magnetic vortex is subject to an external excitation as an oscillating magnetic field<sup>(12), (13)</sup>, spin-waves<sup>(14)</sup> or thermal excitation<sup>(15)</sup>, the vortex core performs a gyrotropic movement with a characteristic frequency. When the core reaches a critical velocity, its polarity is reverted<sup>(14), (16)</sup>. The control of the dynamic properties is fundamental to achieve the dynamic applications of magnetic vortices. The critical velocity is an intrinsic parameter of each material<sup>(17)</sup> while the dimensions of the disk also define the gyrotropic frequency<sup>(18)</sup>.

Some proposed ways to tailor the frequency are the use of exchange-biased bilayers<sup>(16)</sup> or the induction of an in-plane uniaxial anisotropy<sup>(18)</sup>. In the last case, micromagnetic simulations have been used to study the vortex dynamics in disks with uniaxial planar anisotropy induced along the direction of an applied stress, resulting in a decrease of the gyrotropic frequency. Therefore, it is possible to use planar magnetic anisotropy to tailor the dynamic properties of a magnetic vortex. An important issue in order to achieve practical applications is determining the conditions for magnetic vortex formation in anisotropic structures.

Although the vortex structure has been extensively studied in permalloy ( $\text{Ni}_{80}\text{Fe}_{20}$ ) disks<sup>(1), (14), (19), (20)</sup>, that present a null magnetocrystalline anisotropy, there are very few works concerning anisotropic magnetic disks. The existing works are related to dots with diameters between 60 and 600 nm<sup>(21), (22), (23)</sup>. The only article regarding disks in the micron scale is about Fe-V, a material that exhibits four-fold magnetic anisotropy<sup>(24)</sup>. Here we propose to study the influence of in-plane magnetic anisotropy in vortex formation by comparing experimental and simulation results for  $\text{Co}_{60}\text{Fe}_{40}$  and permalloy (Py) disks in the limit of micron-sized disks.

## 2 Results

The micromagnetic simulations were performed using OOMMF (NIST)<sup>(25)</sup> code that applies the Landau-Lifshitz-Gilbert equation to simulate the spin configuration and compute the energy and magnetization. The simulated microstructures are Py and  $\text{Co}_{60}\text{Fe}_{40}$  disks with diameters in the range 0.5 and 8  $\mu\text{m}$  and 20 nm thick. The parameters used in the simulations are shown in Table 1. Considering these parameters, the exchange lengths for Py and  $\text{Co}_{60}\text{Fe}_{40}$  are,  $l_{ex} \approx 5.29$  and 4.32 nm, respectively. Therefore, the cell sizes used the simulations are  $5 \times 5 \times 20$  and  $4 \times 4 \times 20$  nm<sup>3</sup>. For the  $z$  direction, the cell size was considered equal to the thickness in order to reduce the simulation time, after some validation tests that confirmed that this does not alter significantly the simulation result.

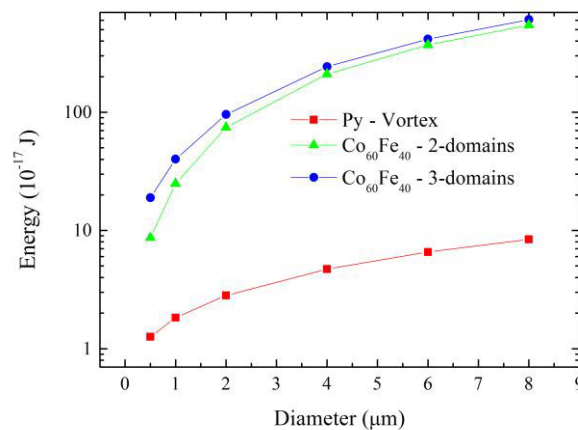
Parameter	Permalloy	$\text{Co}_{60}\text{Fe}_{40}$
Diameter ( $\mu\text{m}$ )	0.5, 1, 2, 4, 6 and 8	0.5, 1, 2, 4, 6 and 8
Thickness (nm)	20	20
Exchange Stiffness - A	$13 \times 10^{-12}$ J/m ( $13 \times 10^{-7}$ erg/cm)	$30 \times 10^{-12}$ J/m ( $30 \times 10^{-7}$ erg/cm)
Saturation Magnetization - $M_s$	$860 \times 10^3$ A/m ( $10.8 \times 10^3$ Oe)	$1600 \times 10^3$ A/m ( $20.1 \times 10^3$ Oe)
Crystalline Anisotropy Constant - $K_l$	0	$-30 \times 10^3$ J/m <sup>3</sup> ( $-300 \times 10^3$ erg/cm <sup>3</sup> )
Anisotropy Direction	---	(100)
Cell Size (nm <sup>3</sup> )	$5 \times 5 \times 20$	$4 \times 4 \times 20$

**Table 1:** Simulation parameters used in the micromagnetic simulations.

For each disk diameter, we made simulations starting from different initial configurations: aleatory; vortex; single-domain in the directions (100), (010), (001), (110) and (111); two-domains in the directions (100) and (010). The definition of coordinate axes ( $xyz$ ) used in this study was:  $x$  = in-plane, horizontal;  $y$  = in-plane, vertical and  $z$  = out-of-plane. A damping constant of 0.5 have been considered in the simulations in order to model the relaxation of the initial configuration. It does not correlated with the actual damping constant of the systems. The most stable configuration for each case have been obtained from the final configuration and the total energy determined by the simulations.

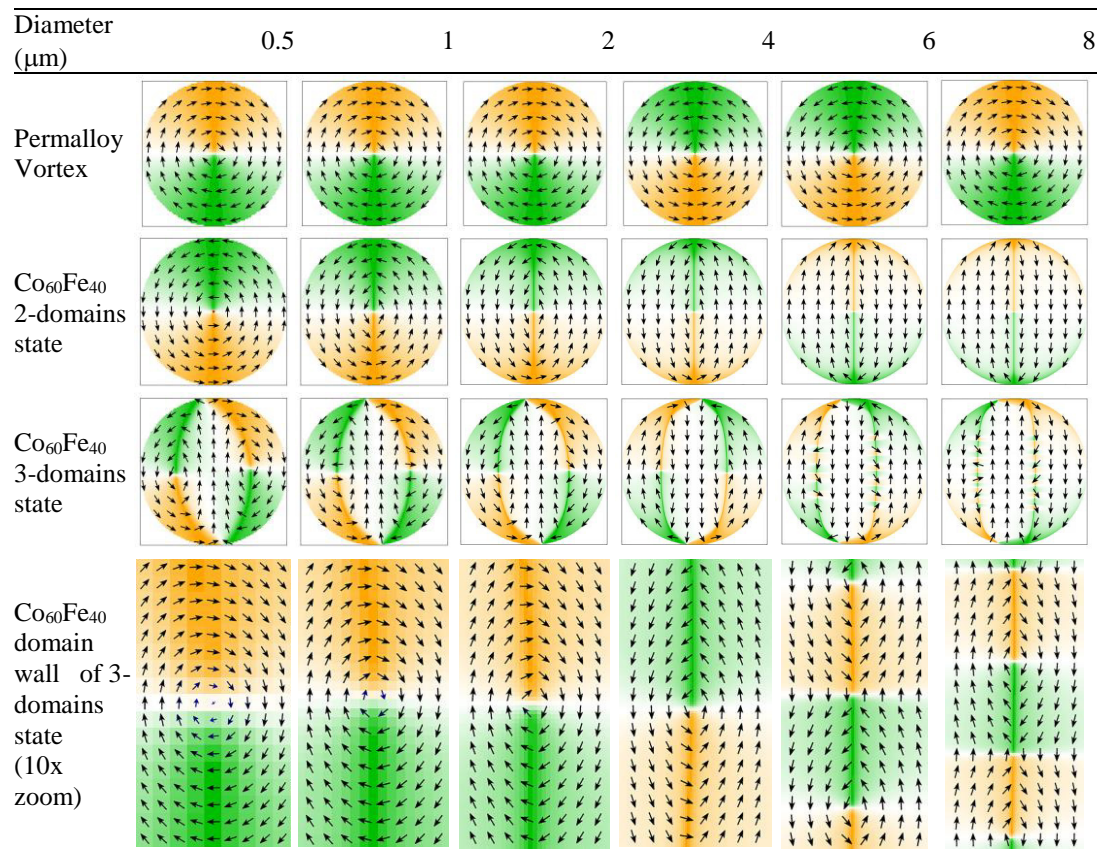
Finally, the simulated configurations were used to calculate MFM images. It was considered that the MFM image is obtained from the phase shift of the tip oscillation that is proportional to the magnetic force gradient or, equivalently, the second derivative of the stray field<sup>(26)</sup>. Approaching the tip as a magnetic dipole, the MFM images were calculated by means of a bi-dimensional Fast Fourier Transform (FFT) of the force gradient obtained from the simulation data.

In the case of the permalloy disks, the lower energy configuration is the vortex state for all the studied sizes. It is confirmed by experimental results found in the literature, were vortex configurations were observed in permalloy disks<sup>(19), (20), (27), (28)</sup>. The vortex is also the lower energy state for  $\text{Co}_{60}\text{Fe}_{40}$ . However the presence of the anisotropy generates a deviation on the vortex circular symmetry, leading to the formation of two regions with opposite oriented spins. These regions increase with the increase of the disk diameter until the formation of a two-domain state, as can be observed in Table 2. Moreover, due to the magnetic anisotropy, a division in three domains can also occur. It was observed that the difference in the calculated energy of the two magnetic configurations for the  $\text{Co}_{60}\text{Fe}_{40}$  disks decrease with increasing disk diameter (see Figure 1).



**Figure 1:** Total energy values obtained from micromagnetic simulations for each spin configuration represented in Table 2.

For the 3-domains configuration zoom in (10x) images of the domain wall have been included in Table 2, and two different domain wall structures were observed. For disks with diameters up to 4  $\mu\text{m}$ , the domain transition occurs through a vortex structure, similarly to what was observed for the 2-domains state. On the other hand, for 6 and 8  $\mu\text{m}$  of diameter, the disks present cross-tie domain walls<sup>(29)</sup> with alternating vortex and anti-vortex structures. This transition do not appear for the 2-domains configuration with the same disk diameter.



**Table 2:** Spin configurations obtained in the micromagnetic simulations representing the lower energy state for permalloy disks and the two lower energy states for  $\text{Co}_{60}\text{Fe}_{40}$  disks. Lower row: Zoom in (10x) of the domain wall center region for the 3-domains state in  $\text{Co}_{60}\text{Fe}_{40}$  disks.

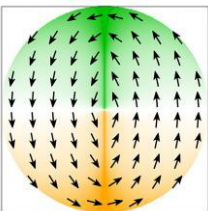
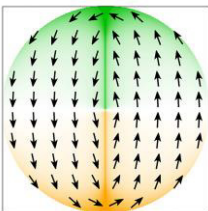
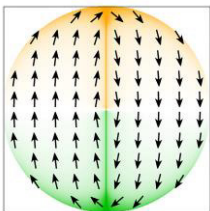
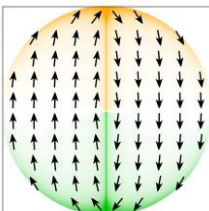
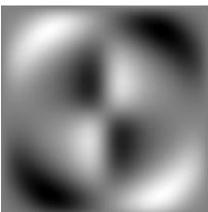
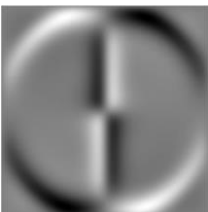
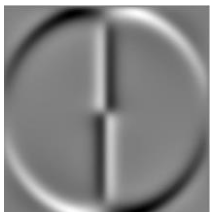

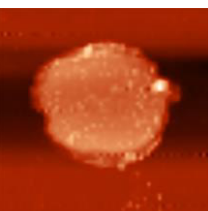
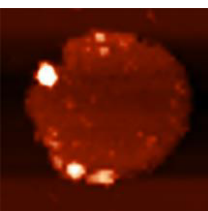
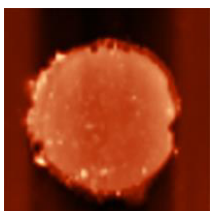

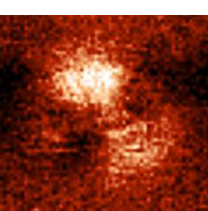
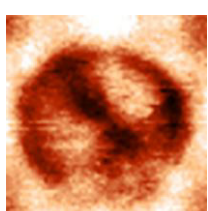

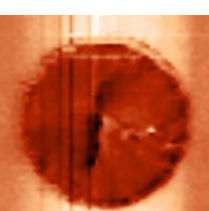
The disks with cross-tie domain wall also have a asymmetric domain structure with the central domain displaced in the x-direction. In the disks where the domain transition happens with a vortex the domain structure is always symmetric for both two and three domains states. Not only the size but also the structure of the domain walls are asymmetric. It can be easily observed in the MFM simulate image in Table 3 and Table 4, the number of vortex/antivortex and their periodicity is different for the two walls in each disks.

The domain wall transition from a single vortex to a cross-tie with multiple vortex/antivortex can be explained by the larger disk size. In the smaller disks the shape anisotropy due to the circular geometry favors the vortex formation. With the decrease of the perimeter/area ratio the disk approaches the continuous film limit and there are more spins aligned in bigger domains. So, the vortex formation is not anymore energetically favorable and a cross-tie domain wall is formed. The minor importance of the geometry can be also the explanation of the formation of displaced domains instead of symmetric ones. In the case of the two-domains configurations, the most symmetric structure makes the vortex wall energetically favorable and no cross-tie domain walls were observed in the simulations.

The MFM measurements were done using a NTEGRA Aura MFM (NT-MDT Co.) and magnetic-coated silicon cantilevers (PPP-MFMR, Nanosensors<sup>TM</sup>) magnetized along the tip axis. The sample consist of an array of non-interacting  $\text{Co}_{60}\text{Fe}_{40}$  disks prepared by a lithographic process. The disks have

thickness of 20 nm, diameters of 2, 4, 6 and 8  $\mu\text{m}$  and center-to-center distance of 4, 8, 12 and 16  $\mu\text{m}$ , respectively. The images obtained were compared with the MFM simulated images.

Although the vortex/two-domains configuration is the lower energy state in all cases, other magnet configurations were also observed. This fact indicates that not all disks are in the lower energy state. For all disks sizes, vortex and three domains, configurations appeared in MFM images, as can be observed in Table 3 and Table 4. This happens due to the small energy difference between these configurations. However, the proportion of each configuration changes according the disk size.

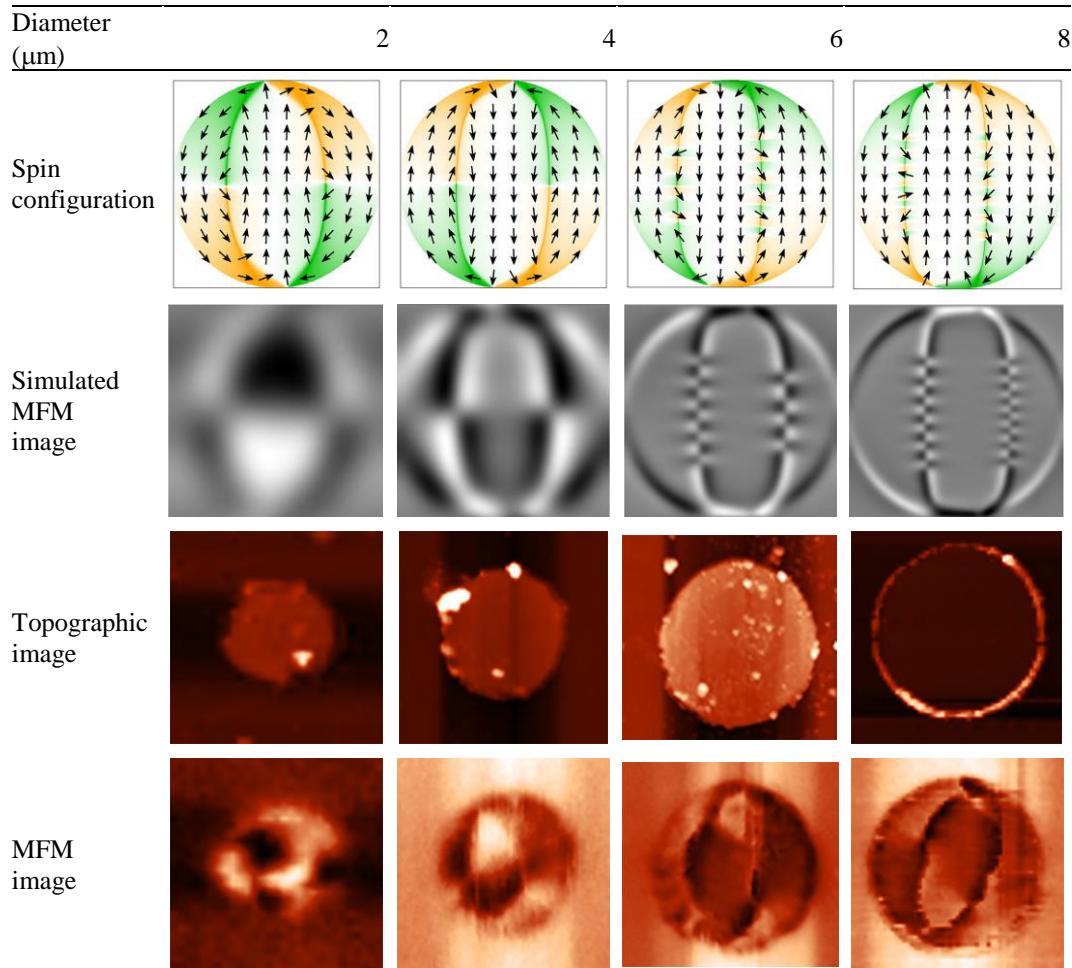
Diameter ( $\mu\text{m}$ )	2	4	6	8
Spin configuration				
Simulated MFM image				
Topographic image				
MFM image				

**Table 3:** From top to bottom: calculated spin configuration and MFM images, measured topographic and magnetic images for  $\text{Co}_{60}\text{Fe}_{40}$  disks showing the evolution from vortex to 2-domains configuration with disk diameter.

The 2-domains configuration observed in the MFM measurements is equivalent to the simulations for all disks sizes, always presenting two symmetric domains. In the case of the 3-domains state, the asymmetric domains appears in the 4  $\mu\text{m}$  disks rather than the 6  $\mu\text{m}$ , as observed in the simulations results. As this size is near the transition between the two situations and the experimental disks are not perfect as the simulated, the defects existent in the sample can induce this asymmetry in smaller disks.

Considering the domain wall structures, the resolution of our MFM images is not enough to have a clear distinction between the two kinds of domain walls observed in the simulations (central vortex

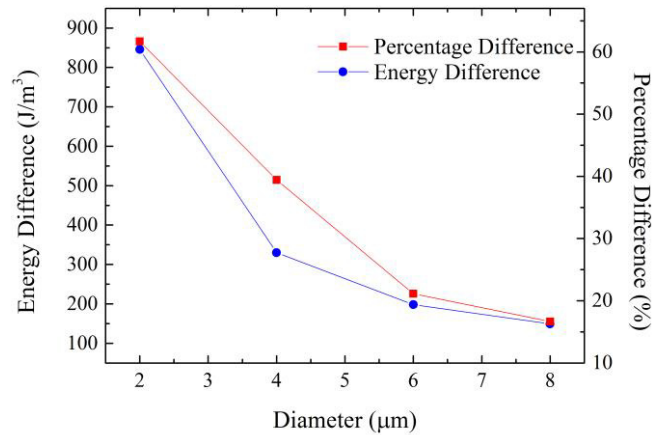
or cross-tie wall). However, it seems that the transition occurs by means of a single vortex even for the 8  $\mu\text{m}$  disks. If this is the case, one reason could be due to structural defects in the real samples that changes the energy equilibrium favoring a different structure when compared with the idealized simulated disks.



**Table 4:** From top to bottom: calculated spin configuration and MFM images, measured topographic and magnetic images for  $\text{Co}_{60}\text{Fe}_{40}$  disks showing the evolution of 3-domains configuration with disk diameter.

The statistical distribution of the magnetic configuration has been determined by a series of statistical measurements totaling 180 disks for each diameter and the results are presented in Figure 2. The graphic shows the percentage difference between the 2-domains and 3-domains configurations (right axis). The difference is bigger for the smallest disks and decrease with the increase of disks sizes. Therefore, it suggests that magnetocrystalline anisotropy favors multidomain formation. Figure 2 also presents the energy density difference between these two configurations (left axis). The scale of right and left axes were arbitrarily chosen to coincide the first and the last points, aiming to facilitate the comparison. It exhibits similar tendency of reduction of the difference with the increase of the disk diameter. This result suggests that the relative probability difference of the magnetic configurations is

determined by the energy density difference, which is in agreement with the observation from Cherifi et al. <sup>(30)</sup> for mesoscopic Co structures.



**Figure 2:** Percentage difference and energy density difference between vortex/two-domains and three domains configuration.

### 3 Conclusions

The aim of this work was study the effect of planar magnetocrystalline anisotropy in the magnetic vortex configuration. Permalloy and  $\text{Co}_{60}\text{Fe}_{40}$  disks have been studied using micromagnetic simulations. According to the simulation results the magnetic vortex is always the low energy state for the permalloy disks, which was confirmed by experimental results found in the literature. However, for the  $\text{Co}_{60}\text{Fe}_{40}$  disks the lower energy state is similar to the vortex state with a deviation from the circular symmetry, that increases with the disk diameter leading to the formation of a two-domains state for larger disks with a central vortex in the domain wall. Furthermore, a three-domains configuration have a lightly higher energy and the energy difference between these states decreases with the diameter increase. So, the anisotropy favors the spins alignment and domains division, reducing vortex stability. Moreover, the micromagnetic calculations show that there are two different domain wall structures in the three-domains state, depending on disk diameter: up to  $4 \mu\text{m}$  the domain transition occurs through a single vortex as in the two-domains states. However, for bigger diameters a cross-tie domain wall is formed by the alternation of vortex and antivortex. The energy difference between these two configurations decrease with the diameter increase, due to the smaller perimeter/area ratio that reduces the effect of the shape anisotropy due to the circular geometry.

In addition, the magnetic configuration of non-interacting  $\text{Co}_{60}\text{Fe}_{40}$  disks have been investigated by using MFM. Although the vortex/two-domains is the lower energy state, the MFM results showed also a significant number of disks in the three-domains state. This happens due to the small energy difference between those configurations. A cursory statistical analysis of the magnetic configuration distribution indicates that the percentage difference of the disks in each state is proportional to the energy difference between the states.

## Acknowledgments

The authors would like to acknowledge the support of the Brazilian agencies CAPES, CNPq, and FAPEMIG.

## References

1. **Chien, C.L., Zhu, Frank Q. and Zhu, Jian-Gang.** *Physics Today*. 2007, Vol. 60, pp. 40-45.
2. **Novais, E.R.P., et al.** *Journal of Applied Physics*. 2011, Vol. 110, 053917.
3. **Martín, J.I., et al.** *Journal of Magnetism and Magnetic Materials*. 2003, Vol. 256, pp. 449-551.
4. **Lehndorff, R., et al.** *Physical Review B*. 2009, Vol. 80, 054412.
5. **Devolter, T., et al.** *Applied Physics Letters*. 2010, Vol. 97, 072512.
6. **Bohlens, S., et al.** *Applied Physics Letters*. 2008, Vol. 93, 142508.
7. **Pigeau, S., et al.** *Applied Physics Letters*. 2010, Vol. 96, 132506.
8. **Hamadeh, A., et al.** *Physical Review B*. 2014, Vol. 112, 257201.
9. **Kim, D.H., et al.** *Nature Materials*. 2010, Vol. 9, pp. 165-171.
10. **Rozhkova, E.A., et al.** *Journal of Applied Physics*. 2009, Vol. 105, 07B306.
11. **Leulmi, S., et al.** *Applied Physics Letters*. 2013, Vol. 103, 132412.
12. **Mesler, B.L., et al.** *Journal of Applied Physics*. 2012, Vol. 111, 07D311.
13. **Shim, J.H., et al.** *Applied Physics Letters*. 2011, Vol. 99, 142505.
14. **Kammerer, M., et al.** *Nature Communications*. 2011, Vol. 2, 279.
15. **Machado, T.S., Rappoport, T.G. and Sampaio, L.C.** *Applied Physics Letters*. 2012, Vol. 100, 112404.
16. **Parreiras, S.O., et al.** *Journal of Applied Physics*. 2013, Vol. 114, 203903.
17. **Lee, K.S., et al.** *Physical Review Letters*. 2008, Vol. 101, 267206.
18. **Roy, P.E.** *Applied Physics Letters*. 2013, Vol. 102, 162411.
19. **Shinjo, T., et al.** *Science*. 2000, Vol. 289, pp. 930-932.
20. **Schneider, M., et al.** *Journal of Applied Physics*. 2002, Vol. 92(3), pp. 1466-1472.
21. **Hanson, M., et al.** *Journal of Magnetism and Magnetic Materials*. 2001, Vol. 236, pp. 139-150.
22. **Mejía-López, J., et al.** *Journal of Applied Physics*. 2006, Vol. 100, 104319.
23. **Ivanov, Yu.P., et al.** *Physics of the Solid State*. 2010, Vol. 52(8), pp. 1694-1700.
24. **Mitsuzuka, K., et al.** *Applied Physics Letters*. 2012, Vol. 100, 192406.
25. **Donahue, M.J. and Porter, D.G.** <http://math.nist.gov/oommf/>. [Online]
26. **Barthelmeß, M., et al.** *Journal of Applied Physics*. 2004, Vol. 95, 10, pp. 5641-5645.
27. **Okuno, T., et al.** *Journal of Magnetism and Magnetic Materials*. 2002, Vol. 240, pp. 1-6.
28. **Pulwey, R., et al.** *IEEE Transactions on Magnetics*. 2001, Vol. 37(4), pp. 2076-2078.
29. **McCordy, J. e Schäfer, R.** *New Journal of Physics*. 2009, Vol. 11, p. 083016.
30. **Cherifi, S., et al.** *Journal of Applied Physics*. 2005, Vol. 98, 043901.